

Topical delivery of anthramycin I. Influence of neat solvents

Tasnuva Haque^a, Khondaker M. Rahman^b, David E. Thurston^b, Jonathan Hadgraft^a, Majella E. Lane^a

^aUCL School of Pharmacy, 29-39 Brunswick Square, London, WC1N 1AX

^bInstitute of Pharmaceutical Science, King's College London, Britannia House, 7 Trinity Street, London, SE1 1DB

Abstract

Anthramycin (ANT) was the first pyrrolobenzodiazepine (PBD) molecule to be isolated, and is a potent cytotoxic agent. Although the PBD family has been investigated for use in systemic chemotherapy, their application in the management of actinic keratoses (AK) or skin cancer has not been investigated to date. In the present work, anthramycin (ANT) was selected as a model PBD compound, and the skin penetration of the molecule was investigated using conventional Franz diffusion cells. Finite dose permeation studies of ANT were performed using propylene glycol (PG), 1,3-butanediol (BD), dipropylene glycol (DiPG), Transcutol P® (TC), propylene glycol monocaprylate (PGMC), propylene glycol monolaurate (PGML) and isopropyl myristate (IPM). The skin penetration of BD, DiPG, PG and TC was also measured. Penetration of ANT through human skin was evident for TC, PG and PGML with the active appearing to “track” the permeation of the vehicle in the case of TC and PG. Deposition of ANT in skin could be correlated with skin retention of the vehicle in the case of IPM, PGMC and PGML. These preliminary findings confirm the ability of ANT to penetrate human skin and, given the potency of the molecule, suggest that further investigation is justified. Additionally, the findings emphasise the critical importance of understanding the fate of the excipient for the rational design of topical formulations.

Keywords

Skin cancer, anthramycin, pyrrolobenzodiazepines, PBDs, solvents, permeation, Franz diffusion cell, topical therapy

1. Introduction

Because of their relative lack of pigmentation Caucasian populations are at a much higher risk of suffering from non-melanoma and melanoma skin cancers than darker skinned ethnic groups (Diepgen and Mahler, 2002). Today, skin cancer is also the most common cancer in individuals with lighter skin tones (Byrd-Miles et al., 2007). The disruption of deoxyribonucleic acid (DNA) in skin cells by ultraviolet (UV) radiation is the initial step in development of skin cancer. Subsequently, DNA repair mechanisms are not activated and the neoplasm progresses. Initially the cancer develops in the outer skin layers and may progress and metastasise to deeper locations in the tissues. It has been proposed that the appearance of actinic keratoses (AKs) or solar keratoses on the skin is the earliest sign of skin cancer (Ibrahim and Brown, 2009). AKs are usually scaly or crusty growths and develop because of chronic skin damage associated with sun exposure. Treatment options for skin cancer include surgery, systemic or topical chemotherapy, radiation, photodynamic light therapy, immunotherapy and targeted therapy. Topical chemotherapy has been used in the management of AKs and non-melanoma skin cancers rather than melanoma, because of the aggressive nature of the latter (Erickson and Miller, 2010). The advantage of topical delivery is that most of the drug is delivered to the site of the lesion and thus there are far fewer side-effects compared with oral or intravenous administration. To date, there are very few agents used for topical chemotherapy, and these include 5-fluorouracil, imiquimod, diclofenac sodium, ingenol mebutate and alitretinoin (Haque et al., 2015).

Pyrrrolobenzodiazepines (PBDs) are sequence-selective minor groove DNA-interacting antitumour agents. Anthramycin (ANT) was the first compound of the pyrrolobenzodiazepine (PBD) group to be identified. It was obtained from a natural source, namely a thermophilic actinomycete (*Streptomyces refuineus*) in 1963 (Tendler and Korman, 1963). A fermentation

broth containing ANT was found to inhibit sarcoma 180 and adenocarcinoma 755 tumours to a significant extent (Leimgruber et al., 1965a; Tendler and Korman, 1963). The active compound was isolated by Berger and co-workers, and the structure determined to be 5,10,11,11a-tetrahydro-9,11-di-hydroxy-8-methyl-5-oxo-1H-pyrrolo[2,1-c][1,4]benzodiazepine-2acrylamide (see Table 2). The generic name ‘anthramycin’ was proposed based on its structural similarity to anthranilic acid (Leimgruber et al., 1965a; Leimgruber et al., 1965b). ANT (the N10-C11 carbinolamine form) may also be isolated as the equivalent anthramycin N10-C11 methyl ether or as anhydroanthramycin depending on the solvent used to dissolve or crystallise the compound. However, the biological activities of the three forms of ANT are equivalent as once dissolved in aqueous media (e.g., biological fluids) the carbinolamine form is predominant (Adamson et al., 1968; Leimgruber et al., 1965a; Leimgruber et al., 1965b). In animal models, ANT exhibited significant positive antitumour activity when given subcutaneously once daily (0.10 mg/kg/d) for a total of 8 doses against human epidermoid carcinoma (H. Ep. No. 3) in conditioned weanling rats (Grunberg et al., 1966). ANT inhibits RNA and DNA synthesis, with preferred binding to double-stranded DNA rather than single stranded DNA (Kohn et al., 1968). The carbinolamine form of ANT was found to be the reactive group that predominantly binds to DNA. However, ANT causes very little disruption of the DNA double-helix (Hurley and Petrussek, 1979; Petrussek et al., 1981). The ANT-DNA adduct prevents further nucleic acid synthesis and therefore, cell division.

Zbinden and co-workers showed that ANT exhibited dose-dependent cardiotoxicity (Cargill et al., 1974). Therefore, despite its potent cytotoxic properties and antitumour effects, it was not developed further as an anticancer drug. More recently, members of the PBD family have been developed as cytotoxic payloads for attachment to antibodies to form Antibody-Drug Conjugates (ADCs), and a number of these are presently in the clinic for the

treatment of various leukaemias and lung cancer (Mantaj et al., 2017). However, the administration of ANT, other than *via* the systemic route, has not been investigated to date. Therefore, the aims of the present work were (i) to investigate the suitability of ANT for topical delivery, and (ii) to identify suitable vehicles for targeting of ANT to the skin. If effective amounts of ANT penetrate the skin, the potential to progress the molecule as a topical chemotherapeutic agent may be explored further. As reported previously, vehicle selection was based on an assessment of solubility parameter values of various solvents and solubility determination (Parisi et al., 2016).

2. Materials and methods

2.1 Materials

ANT was purchased from Sigma Aldrich, UK. Propylene glycol (PG), isopropyl myristate (IPM) and acetone were supplied by Sigma Aldrich, UK. Transcutol[®] (TC), Capryol 90[®] or propylene glycol monocaprylate (PGMC) Type II and Lauroglycol 90[®] or propylene glycol monolaurate (PGML) Type II were obtained from Gattefossé, France. Dipropylene glycol (DiPG) and n-octanol (99% pure) obtained from Acros Organics (UK). 1,3-butanediol (BD) was purchased from Wako Pure Chemical Industries Ltd., Japan. High Performance Liquid Chromatography (HPLC) grade water, methanol, acetonitrile, and trifluoroacetic acid (TFA) were purchased from Fisher Scientific, UK. For gas chromatography (GC) analysis, 1,2-butanediol (>98% pure, internal standard for PG) and phenylboronic acid ($\geq 97\%$ pure, a derivatising agent for both PG and BD) were supplied by Fluka (Sigma Aldrich, Japan) and Fluka (Sigma Aldrich, UK), respectively. To prepare the receptor medium, phosphate-buffered saline (PBS) tablets (Dulbecco A, Oxoid Limited, UK),

deionised water (Elga water purifier, UK) and sodium azide (Fluka, Sigma Aldrich, UK) were used.

2.2 Log P, solubility parameter calculation, solubility and stability

The Log P value for ANT was determined experimentally using the shake flask method with n-octanol and water (United States Environmental Protection Agency, 1996); Log P values for the solvents were calculated using ChemBioDraw® Ultra (Version 12.0) software (PerkinElmer, USA). Solubility parameters for ANT and vehicles were calculated using Molecular Modelling Pro® (Version 6.3.3) software (ChemSW, Fairfield, CA, USA).

Solubility studies were conducted by adding a large excess of ANT into a fixed volume of solvent in an Eppendorf® tube. The tubes were capped and sealed with Parafilm®. The tubes were shaken for 10 min using a vortex shaker (IKA® Vortex Genius 3, UK). A rotor (Stuart, UK) was placed inside a temperature-controlled oven (Jouan, France). The oven temperature was set at $32\pm 0.5^{\circ}\text{C}$. The Eppendorf® tube was placed in the rotor, rotating at 40 rpm and left for 48 h. At the end of the study, the tube was centrifuged at 13,000 rpm, at 32°C and for 20 min (Centrifuge 5415R, Eppendorf, Germany). The supernatant portion was collected and diluted sufficiently for HPLC analysis. The experiments were conducted in triplicate.

The stability studies were conducted by dissolving known quantities of ANT in neat solvents (n=3). The vials were shaken for 5 min to ensure mixing of the compounds in the solvent and then filtered using a Millex® GP filter unit (0.22 μm , Millipore Express®, Ireland). The solution was placed in a glass vial, capped and sealed using Parafilm® and

placed in a water bath at $32\pm 0.5^{\circ}\text{C}$. Samples were collected at 0, 24 and 48 h, diluted if necessary, and analysed by HPLC as described in the next section.

2.3 HPLC analysis

A Hewlett Packard series 1050 HPLC machine (USA) with a variable wavelength UV-VIS detector was used to analyse ANT, with a Waters Sunfire (UK) C_{18} column (250×4.6 mm, $5\ \mu\text{m}$ packing particle size). Data were collected at a detection wavelength of 240 nm using Prime® (Version 4.2.0) software. The mobile phase consisted of water (0.1% TFA):methanol (50:50). The flow rate of the mobile phase was 1 ml/min and the injection volume was 20 μl . Under these conditions the retention time of ANT was 6.4 min. Standard solutions of ANT in methanol were prepared in the range of 1.1 to 88 $\mu\text{g/ml}$. A good correlation ($r^2>0.99$) was observed between the concentration and the respective peak area, with an accuracy value of $100.97\pm 3.56\%$. The relative standard deviation (%RSD) values of intra- and inter-day precision were ≤ 3.1 . The limit of quantitation was 1.1 $\mu\text{g/ml}$.

2.4 GC analysis

The GC system (7890A, Agilent Technologies) consisted of an auto sampler and an injector. Nitrogen was used as the carrier gas and detection was conducted with a flame ionisation detector (FID). Two capillary columns were used for the selected solvents (Table 2): Ultra 1® (Dimethyl polysiloxane, Agilent Technologies, J & W Scientific, USA) with 25 m length, 0.20 mm internal diameter and $0.33\ \mu\text{m}$ film thickness and an HP 5® [(5%-Phenyl)-methyl polysiloxane, Agilent J & W GC column, USA] with a length of 30 m, internal diameter of 0.32 mm and a film thickness of $0.25\ \mu\text{m}$. The temperature range of both

columns was -60°C to 325°C . Data were recorded and analysed with Agilent Open Lab CDS Chemstation® software. The GC methods are given in detail in Table 2. PG and BD are polar short chain glycols (Li et al., 2007), and derivatisation was required to increase their peak detection and sensitivity. PG and BD were derivatised with 40 mmol phenylboronic acid in acetone (Ehlers et al., 2013; Porter and Auansakul, 1982). The sample and standard preparation method of PG was adapted from Santos *et al.* (Santos et al., 2009). The internal standards for PG and BD were 1, 2 butanediol in methanol ($0.6\ \mu\text{mol/ml}$) (Santos et al., 2009) and n-octanol in acetonitrile ($0.6\ \text{g/l}$) (Blanchet et al., 2002), respectively. $50\ \mu\text{l}$ of standard solution or sample of either PG or BD and $50\ \mu\text{l}$ of internal standard were placed in an Eppendorf® tube. After mixing, $50\ \mu\text{l}$ of this mixture were taken in another Eppendorf® tube and $50\ \mu\text{l}$ of derivatising agent were added and mixed immediately before injection. Calibration curves were constructed and samples were analysed by taking the ratios of the peak areas of the solvents and their respective internal standards. The accuracy value for all the solvents was within the range of $100\pm 4\%$. The RSD values of intra- and inter-day precision were less than 2.20% and 5%, respectively.

2.5 Dynamic vapor sorption studies

In order to examine the evaporation of candidate vehicles, a Dynamic Vapor Sorption (DVS) instrument (Surface Measurement Systems Ltd., Marlow, UK) was used. Nitrogen was used as a carrier gas, with a flow rate at $200\ \text{ml/min}$. The samples were analysed at 32°C and at 50% relative humidity (R.H.) for 48 h. $10\ \mu\text{l}$ of neat solvent were applied to the sample pan. The pan was then stabilised for approximately 2 min. The weight of the applied solvent was then fixed as the initial weight (mg) and the experiment started. The software recorded

the readings (or weight of the sample gravimetrically) up to 48 h. The change in mass was calculated by the following formula

$$\% \text{ of initial weight} = \frac{\text{Final mass (mg)} \times 100}{\text{Initial mass (mg)}} \dots \dots \dots \text{Equation 1}$$

2.6 Finite dose permeation and mass balance studies

‘Franz’-type vertical glass diffusion cells were used for the ANT permeation studies in human skin as reported previously (Oliveira et al., 2012a). Following informed consent and ethical approval (Research Ethics Committee reference 07/H1306/98), human skin was obtained from the abdomen of donors who had undergone surgery. The viable epidermis was prepared from Caucasian female abdominal full thickness skin by the heat separation method. (Kligman and Christophers, 1963). PBS solution was prepared by dissolving ten PBS tablets in 1 litre of deionised water (pH 7.30±0.10). As the experiment was conducted for 48 h, 0.002% (w/v) sodium azide was used with the PBS solution. Degassed receptor solution was used as the receptor compartment. The area of diffusion area was accurately measured (0.8-1.1 cm²). The surface temperature was confirmed to be 32±0.5°C (TM-22 Digitron digital thermometer, RS Components, Corby, UK). A 10 µl aliquot of the saturated drug solution was applied in the donor compartment and spread carefully to cover the exposed surface. 200 µl of receptor solution were withdrawn at different time intervals up to 48 h and the same amount of fresh temperature equilibrated receptor solution was added to replace the sample. At the end of the study, ANT and solvents were analysed by HPLC and GC, respectively.

After the 48 h permeation study, the receptor medium was removed completely. The mass balance study was conducted and validated. The skin surface was washed twice with 1 ml of methanol and three times with 1 ml of methanol-water (50:50) mixture. The skin was

removed from the Franz cell and placed in an Eppendorf® tube with 1 ml of methanol. All the tubes were placed in a rotor (rotating at 40 rpm) in a temperature-controlled oven ($32\pm 0.5^{\circ}\text{C}$) for 3 h. After extraction was completed, the tube was centrifuged at 13,000 rpm at 32°C for 15 min. Aliquots were taken from the supernatant portion and analysed by HPLC and GC in order to quantify the amounts of ANT and respective solvents on the surface of the skin and inside the skin.

2.7. *Statistical analysis*

Data analysis was conducted with MS Excel® 2007, and the results were presented as mean \pm SD (standard deviation). IBM SPSS Statistics software (version 22.0) was used for statistical evaluation. The Shapiro-Wilk test was used to check the normality of the results. If the p value calculated from the test was greater than 0.05, the data were assumed to be normally distributed (parametric). One way analysis of variance (ANOVA) was done as a parametric test. Multiple comparisons between each individual group were performed by the post hoc Tukey test. For non-parametric data, Kruskal-Wallis one way ANOVA followed by multiple comparisons between groups was performed. Equal variance was assumed in all cases. $p < 0.05$ was considered as the statistical significant difference.

3. **Results and discussion**

3.1 *Log P, solubility parameter, solubility and stability studies*

The physicochemical properties of ANT are shown in Table 2. ANT is a yellow powder with a relatively low molecular weight (315.32 Da). The $\log P$ was determined to be 1.15 ± 0.83 and the reported melting point is 188-194°C (Leimgruber et al., 1965a). The calculated physicochemical parameters of the solvents are listed in Table 2. The first three solvents were selected primarily because of the proximity of their solubility parameters to that of ANT [$15.35 \text{ (cal/cm}^3)^{1/2}$]. PG, BD and DiPG are low molecular weight hydrophilic solvents; TC is also a hydrophilic solvent with a solubility parameter close to that proposed for skin, $10 \text{ (cal/cm}^3)^{1/2}$ (Liron and Cohen, 1984). PGMC, PGML and IPM are hydrophobic solvents with solubility parameters that are also similar to that for human skin, and predicted $\log P$ values are 2.5, 4.17 and 5.86, respectively. IPM is a well-known skin penetration enhancer used in topical and cosmetic products (Lane, 2013). PGML is used in transdermal and cosmetic products (Fenton and Rowe, 2013c). PGMC has not been investigated as a penetration enhancer in human and porcine skin models to date.

The solubilities for ANT in the various vehicles are shown in Table 4, with the highest values observed for PG followed by BD, DiPG and TC. The solubility of ANT ranged from 1 - 10 mg/ml in PGML, PGMC and water, and the lowest value was observed in IPM. It has previously been hypothesised that the lower the solubility parameter difference between a solute and solvent, the higher the solubility of the solute in that solvent (Florence and Attwood, 2006). This appears to be the case in the present work with PG, BD and DiPG; PG and BD had the closest solubility parameter to ANT and therefore, the solubilities of ANT in these solvents were higher compared with the other solvents. As the difference between solvent and solute solubility parameter values increases, solubility decreases. PGMC and PGML have similar solubility parameter values, (Table 1), and the solubility of ANT in these solvents was ~5.6 mg/ml. ANT solubility was lowest in IPM and water, because of the high difference in solubility parameter values; the solubility parameter of water is 22.97

(cal/cm³)^{1/2}. After 48 h stability studies at 32°C, the recovery of ANT in all solvents was >89%, with the exception of TC where ~70% ANT was recovered; ANT also demonstrated instability in PBS (data not shown).

3.2 Solvent evaporation studies

The results for the DVS studies of the candidate vehicles are shown in Figure 1. There was complete evaporation of TC and PG by 16 and 37 h, respectively. For BD, 70.3% of the applied mass was recovered at 48 h. Only 13% of the applied DiPG evaporated during the experiment. More than 94% of the applied weights of PGMC, PGML and IPM were recovered at the end of the experiment. PG, TC, BD and DiPG also absorbed water at early time points. The value for equilibrium vapour pressure is indicative of the evaporation rate of a vehicle or liquid, and a liquid with a high vapour pressure is considered to be volatile (Sinco and Singh, 2011). The vapour pressure of TC is higher than PG and BD (Table 3), consistent with the faster evaporation of TC (100% evaporation at 16 h) compared with PG and BD. Similarly, DiPG showed comparatively low volatility because of the lower vapour pressure value reported for this solvent (Table 3). The vapour pressure of PGMC and PGML is not reported in the literature, and the vapour pressure of IPM is very low - 9.35×10^{-5} mm Hg (Daubert and Danner, 1989); the DVS data confirm that these solvents are not volatile (Figure 1).

3.3 Permeation and mass balance studies - ANT

Finite dose permeation studies of ANT were performed using PG, BD, DiPG, TC, PGMC, PGML and IPM. A dose equivalent to 10 µl (8.5 - 11.2 mg) of vehicle was applied

on the surface of the skin. Permeation of ANT was only observed for PG, TC and PGML; permeation profiles are shown in Figures 2a and 2b. Precipitation of ANT was also evident in the donor chamber for both PG and TC during the course of the permeation study. Figure 2a shows that, at 48 h, the highest amount of ANT permeated from TC ($17.6 \mu\text{g}/\text{cm}^2$) followed by PG ($12.5 \mu\text{g}/\text{cm}^2$) and PGML ($8.5 \mu\text{g}/\text{cm}^2$). The values were not significantly different from each other ($p>0.05$). A curvilinear permeation profile of ANT in TC is also evident in Figure 2a. Permeation of ANT in PG and PGML was not detected until 5 and 8 h, respectively with similar permeation profiles up to 32 h. As a dose equivalent to $10 \mu\text{l}$ of a saturated solution of ANT in the different vehicles was applied, the percentage ANT permeation as a function of time is shown in Figure 2b. Although the cumulative amount of ANT that permeated was the lowest for PGML, the percentage permeation at 48 h was highest (13.1%) for this vehicle compared with the PG (0.6%) and TC (8.0%). The ability of PGML to act as a skin penetration enhancer has been reported previously (Hirata et al., 2013; Mohammed et al., 2014; Parisi et al., 2016). It has been suggested that the presence of unesterified lauric acid in PGML may contribute to increased membrane permeation. The percentage ANT permeation at 48 h for PG is significantly lower compared with TC and PGML ($p<0.05$).

The results for mass balance studies and permeation of ANT are shown in Table 5. ANT was retained inside the skin in high quantities for PG, PGMC and TC and the amounts were not significantly different ($p>0.05$). For PGML and BD, amounts of ANT recovered were 2.6 and $2.0 \mu\text{g}/\text{cm}^2$ respectively; application in DiPG and IPM resulted in $1.5 \mu\text{g}/\text{cm}^2$ of ANT retention in the skin. No significant differences were evident in the amounts of ANT extracted from the skin for TC, BD, DiPG, PGMC, PGML and IPM ($p>0.05$). Most of the applied dose of ANT was recovered from the donor compartment. Total amounts for ANT permeation and retention in skin were highest for PG and TC (38 and $27 \mu\text{g}/\text{cm}^2$,

respectively, $p > 0.05$) and the value for PG is significantly higher than for the other solvents ($p < 0.05$). Comparatively lower permeation and retention was evident for PGMC and PGML ($\sim 11 \mu\text{g}/\text{cm}^2$) compared with PG; the corresponding values for the remaining solvents were $> 6 \mu\text{g}/\text{cm}^2$. ANT in IPM could not be quantified from the surface washings because of the low ANT solubility in IPM. The value for percentage skin retention of ANT for the IPM vehicle was relatively high (59.2%) as the applied dose of ANT was low and significantly higher than for the other solvents ($p < 0.05$). Despite high retention of ANT inside the skin for PG (Table 5), the percentage retention was very low (1.3%) because of the comparatively high dose applied. The second highest retention was obtained for ANT in PGMC (17.50%). The percentage retention of ANT for PGMC (17.5%) was significantly higher compared with PG, BD, TC, DiPG, water and PGML. TC and PGML showed similar values for percentage ANT retained in skin ($p > 0.05$), namely 4.43 and 4.01%, respectively; BD and DiPG deposited comparable percentages of ANT ($< 0.3\%$). The total recovery after mass balance ideally should be $100 \pm 15\%$ (Scientific Committee on Consumer safety, 2010). The total recovery of ANT for PG, TC and IPM was 82, 84 and 59%, respectively, while values for solvents where there is no permeation all fall within recommended recovery limits. This reflects the partial degradation of ANT in the receptor phase as noted above.

3.4 Permeation and mass balance studies – solvents

The hydrophobic vehicles (PGMC, PGML and IPM) were not detected in the receptor medium. The permeation profiles of the hydrophilic vehicles are shown in Figure 3. TC permeated through the skin in significantly higher quantities compared with the other solvents ($p < 0.05$). The permeation of TC reached a plateau at 19 h (53.4%); at 48 h, a total of 56.8% of the applied amount had permeated. The second most permeable vehicle was PG,

with a significantly higher percentage permeation at 48 h compared with BD and DiPG ($p < 0.05$). After 27 h, the permeation of PG appeared to plateau and at 48 h, 21.9% of the applied dose had permeated. Thus, at the end of the permeation study, PG permeation was almost 2.5-fold lower than TC ($p < 0.05$). The permeation profiles of BD and DiPG across human skin were similar and final amounts permeated were 10.3% and 8.0%, respectively.

The mass balance results for vehicles after 48 h permeation studies are shown in Figure 4. The percentages of PG and BD recovered from the surface of the skin by washing were 6.9% and 42.4% respectively. No TC was recovered from the skin surface, and this may reflect the comparatively more volatile nature of TC compared with PG and BD (Figure 1). Higher quantities of DiPG, PGMC, PGML and IPM (98.9, 96.6, 95.9 and 65.7% respectively) were obtained from washing the skin surface after the permeation studies compared with PG and BD. The total recovery values of PG and BD were also lower than DiPG, PGMC, PGML and IPM, and this may reflect evaporation of the glycol vehicles. The values for skin retention of IPM, TC and PGMC (11.3, 8.5 and 7.5%, respectively) are significantly higher than all other vehicles ($p < 0.05$), but not significantly different from each other ($p > 0.05$). Corresponding skin retention values for PGML, PG, BD and DiPG were 4.2, 2.1, 1.0 and 2.1%, respectively. Significantly higher amounts of TC permeation and retention are evident (65.3%) compared with the other vehicles ($p < 0.05$). The corresponding value for PG is 24.0%, also significantly higher than the other solvents ($p < 0.05$). Total amounts of permeation and retention for BD, DiPG and IPM were ~10-11% of the applied amounts.

Comparing the permeation profiles of ANT (Figures 2a and 2b) with that for TC, Figure 3), 10% of TC had permeated at 5 h, but ~1% of ANT had permeated by this time point. After 19 h, the TC profile appears to level off, and ANT permeation also shows a plateau. This suggests that the rapid permeation and clearance of TC into the receptor

compartment may result in a deposition of ANT in the skin and no further permeation of ANT in the absence of TC. In contrast, PG permeates more slowly and to a lower extent than TC (Figure 3), but continuous permeation is evident over 48 h as is the case for ANT. PGML was not detected in the receptor phase, but it is the only hydrophobic vehicle to promote skin permeation of ANT, presumably by maintaining the drug in solution in skin over the timeframe of the permeation study.

For the hydrophilic vehicles, TC permeated through human skin to the greatest extent, and more TC was also retained in the skin compared with PG, BG and DiPG. The solubility parameter for TC is similar to the value proposed for skin, and this may contribute to the higher skin uptake and permeation of this vehicle. TC has previously been reported to increase the permeation and retention of various model drugs across the skin (Harrison et al., 1996; Chadha et al., 2011; Oliveira et al., 2012b). High TC skin uptake was also correlated with high uptake of methyl paraben following *in vitro* permeation studies in human skin; higher solvent sorption allows the active to partition more favourably into the skin (Oliveira et al., 2012b). A recent short-angle X-ray scattering (SAXS) study by Moghadam *et al.* showed increased disorder in SC treated for 24 h with TC (Moghadam et al., 2013). However, the amount of TC actually applied to the tissue was not reported, and the experiment may reflect the effects of saturation of the membrane with the solvent rather than finite dose conditions.

PG is used as a solvent and penetration enhancer in many pharmaceutical and cosmetic products and its effects on the stratum corneum have been extensively reviewed (Roussel et al., 2015). Fasano *et al.* investigated the steady state flux of neat PG in an infinite dose study in human skin. These authors estimated that application of a finite dose of PG (10 $\mu\text{L}/\text{cm}^2$) on the skin would result in ~23% dermal absorption at 24 h (Fasano et al., 2011).

However, in the present work, 13% of PG had permeated by 24 h and ~22% of the applied dose of PG had permeated at 48 h (Figure 3). The mechanism of penetration enhancement by PG is still not clear but it has been suggested that PG solvates α -keratin and occupies hydrogen-bonding sites of the SC (Roussel et al., 2015; Lane, 2013). Bouwstra and co-workers (Bouwstra et al., 1991) suggested that PG intercalates with the SC lipid head groups, thus causing a lateral swelling of the lipid alkyl chains by an increase in interfacial area. The recent SAXS study reported by Moghadam et al. (2013) showed that PG did not influence the long or short lamellar spacing of the SC. In general, it is considered that PG may act by increasing the partition or solubility of a drug in the SC (Lane, 2013). Pudney et al. (2007) and Mohammed et al. (2014) used Confocal Raman spectroscopy to investigate the *in vivo* distribution of PG in humans and noted that the depth of penetration of PG correlated well with the active that was applied in the PG vehicle to the forearm. This is consistent with the results observed for the *in vitro* studies in Figures 2 and 3. Low permeation values of BD and DiPG (~8 to 10%) were observed (Figure 3) with no quantifiable permeation of ANT in either of the vehicles. BD permeated to a slightly higher extent (~10%) than DiPG (~8%), whereas as shown in Figure 4 the amount of DiPG deposited inside the skin almost 2-fold higher than for BD (~2 and 1%, respectively). However, ANT deposition inside skin was not significantly different for BD and DiPG. Fasano *et al.* (2011) conducted infinite dose permeation studies with DiPG using human abdominal skin. The flux of DiPG across the skin was almost 3-fold lower than for PG; interestingly, the cumulative flux of DiPG in the present finite dose study is also 3-fold lower than the value for PG. The authors also estimated that if a finite dose is applied ($10 \mu\text{l}/\text{cm}^2$), DiPG might permeate up to 9% at the end of 24 h. Figure 3 shows that the percentage of DiPG permeation was 2.6% at 24 h and 8% at 48 h.

The vehicle-skin retention data showed that IPM and PGMC were retained inside the skin in higher quantities than PGML, and skin retention of these vehicles follows the same trend as skin retention of ANT, namely IPM>PGMC>PGML. Greater partitioning and higher skin retention was demonstrated for IPM compared with alkanols by Goldberg-Cettina et al. (1995). Liu et al. (2009) investigated the effects of IPM on estradiol skin permeation and noted that IPM uptake could be correlated with drug diffusivity in skin. The authors also demonstrated swelling of the SC in the presence of IPM. Oliveira et al. (2012b) also reported a direct dependence of methyl paraben uptake into SC on IPM sorption into the membrane, consistent with the present work.

4. Conclusions

The skin permeation and retention of a model PBD compound, ANT, has been investigated for a range of neat solvents. TC and PGML delivered higher amounts of ANT through the skin compared with the other vehicles. The delivery of ANT clearly “tracked” the skin penetration of TC and, to a lesser extent, PG, emphasising the critical role of the vehicle in the skin delivery of the active. Skin penetration of ANT also mirrored the evaporation of PG and TC. In the management of AK or skin cancer, the active needs to target the outer layers of the skin and thus the lack of permeation observed for certain vehicles does not necessarily rule them out in future formulation development. The stability of ANT warrants further investigation, given some of the low recovery values observed. More complex binary and ternary solvent systems may promote enhanced skin permeation of ANT via synergistic effects, and these will be the subject of a future publication.

Acknowledgements

The authors would like to thank the Commonwealth Scholarship Commission (BDCS-2010-46) for funding the project.

References

Adamson, R.H., Hart, L.G., DeVita, V.T., Oliverio, V.T., 1968. Antitumor activity and some pharmacologic properties of anthramycin methyl ether. *Cancer Res.* 28, 343-347.

Blanchet, B., Morand, K., Hulin, A., Astier, A., 2002. Capillary gas chromatographic determination of 1,4-butanediol and γ -hydroxybutyrate in human plasma and urine. *J. Chromatogr. B.* 769, 221–226.

Bouwstra, J.A., de Vries, M.A., Gooris, G.S., Bras, W., Brussee, J., Ponc, M., 1991. Thermodynamic and structural aspects of the skin barrier. *J. Control. Release.* 15, 209-220.

Byrd-Miles, K., Toombs, E., Peck, G., 2007. Skin cancer in individuals of African, Asian, Latin-American, and American-Indian descent: differences in incidence, clinical presentation, and survival compared to Caucasians. *J. Drugs Dermatol.* 6, 10-16.

Cargill, C., Bachmann, E., Zbinden, G., 1974. Effects of daunomycin and anthramycin on electrocardiogram and mitochondrial metabolism of the rat heart. *J. Natl. Cancer Inst.* 53, 481-486.

Chadha, G., Sathigari, S., Parsons, D.L., Babu, R.J., 2011. In vitro percutaneous absorption of genistein from topical gels through human skin. *Drug Dev. Ind. Pharm.* 37, 498-505.

Daubert, T.E., Danner, R.P., 1989. *Physical and Thermodynamic Properties of Pure Chemicals Data Compilation.* Washington, D.C.: Taylor and Francis.

Diepgen, T., Mahler, V., 2002. The epidemiology of skin cancer. *Br. J. Dermatol.* 146 1-6.

Ehlers, A., Morris, C., Krasowski, M.D., 2013. A rapid analysis of plasma/serum ethylene and propylene glycol by headspace gas chromatography. *SpringerPlus*. 2, 203.

Erickson, C., Miller, S., 2010. Treatment options in melanoma in situ: topical and radiation therapy, excision and Mohs surgery. *Int. J. Dermatol.* 49, 482-491.

Fasano, W.J., ten Berge, W.F., Banton, M.I., Heneweer, M., Moore, N.P., 2011. Dermal penetration of propylene glycols: measured absorption across human abdominal skin in vitro and comparison with a QSAR model. *Toxicol. In Vitro.* 25, 1664-1670.

Fenton, M.E., Rowe, R.C., 2013a. Butylene glycol, In: Rowe, R.C., Sheskey, P.J., Cook, W.G., Fenton, M.E. (Eds.), *Handbook of Pharmaceutical Excipients (Online Edition)*. Pharmaceutical Press and American Pharmacists Association.

Fenton, M.E., Rowe, R.C., 2013b. Dipropylene glycol, In: Rowe, R.C., Sheskey, P.J., Cook, W.G., Fenton, M.E. (Eds.), *Handbook of Pharmaceutical Excipients (Online Edition)*. Pharmaceutical Press and American Pharmacists Association.

Fenton, M.E., Rowe, R.C., 2013c. Propylene glycol monolaurate, In: Rowe, R.C., Sheskey, P.J., Cook, W.G., Fenton, M.E. (Eds.), *Handbook of Pharmaceutical Excipients (Online Edition)*. Pharmaceutical Press and American Pharmacists Association.

Florence, A.T., Attwood, D., 2006. *Physicochemical Principles of Pharmacy*, 4 ed. Pharmaceutical Press, London.

Goldberg-Cettina, M., Liu, P., Nightingale, J., Kurihara-Bergstrom, T., 1995. Enhanced transdermal delivery of estradiol in vitro using binary vehicles of isopropyl myristate and short-chain alkanols. *J. Pharm. Sci.* 114, 237-245.

Grunberg, E., Prince, H.N., Titsworth, E., Beskid, G., Tendler, M.D., 1966. Chemotherapeutic properties of anthramycin. *Chemotherapia*. 11, 249–260.

Haque, T., Rahman, K.M., Thurston, D.E., Hadgraft, J., Lane, M.E., 2015. Topical therapies for skin cancer and actinic keratosis. *Eur. J. Pharm. Sci.* 77, 279-289.

Harrison, J.E., Watkinson, A.C., Green, D.M., Hadgraft, J., Brain, K., 1996. The relative effect of Azone® and Transcutol® on permeant diffusivity and solubility in human stratum corneum. *Pharm. Res.* 13, 542-546.

Hirata, K., Helal, F., Hadgraft, J., Lane, M.E., 2013. Formulation of carbenoxolone for delivery to the skin. *Int. J. Pharm.* 448, 360-365.

Hurley, L.H., Petrusek, R., 1979. Proposed structure of the anthramycin–DNA adduct. *Nature*. 282, 529 - 531.

Ibrahim, F., Brown, M.D. 2009. Actinic keratoses: a comprehensive update. *J. Clin. Aesthet. Dermatol.*, 2, 43-48.

Kligman, A.M., Christophers, E., 1963. Preparation of isolated sheets of human stratum corneum. *Arch Dermatol.* 88, 702-705.

Kohn, K.W., Bono Jr, V.H., Kann Jr, H.E., 1968. Anthramycin, a new type of DNA-inhibiting antibiotic: reaction with DNA and effect on nucleic acid synthesis in mouse leukemia cells. *Biochim. Biophys. Acta.* 155, 121-129.

Ladyzhynsky, N.S., 2013. Propylene glycol, In: Rowe, R.C., Sheskey, P.J., Cook, W.G., Fenton, M.E. (Eds.), *Handbook of Pharmaceutical Excipients (Online Edition)*. Pharmaceutical Press and American Pharmacists Association.

Lane, M.E., 2013. Skin penetration enhancers. *Int. J. Pharm.* 447, 12-21.

Leimgruber, W., Stefanovic, V., Schenker, F., Karr, A., Berger, J., 1965a. Isolation and characterization of anthramycin, a new antitumor antibiotic. *J. Am. Chem. Soc.* (Communications to the Editor). 87, 5791-5793.

Leimgruber, W., Batcho, A.D., Schenker, F., 1965b. The structure of anthramycin. *J. Am. Chem. Soc.* (Communications to the Editor). 87, 5793-5795.

Li, Z., Kozlowski, B.M., Chang, E.P., 2007. Analysis of aldehydes in excipients used in liquid/semi-solid formulations by gas chromatography–negative chemical ionization mass spectrometry. *J. Chromatogr. A.* 1160, 299–305.

Liron, Z., Cohen, S., 1984. Percutaneous absorption of alkanolic acids II: application of regular solution theory. *J. Pharm. Sci.* 73, 538-542.

Liu, P., Cettina, M., Wong, J., 2009. Effects of isopropanol–isopropyl myristate binary enhancers on in vitro transport of estradiol in human epidermis: a mechanistic evaluation. *J. Pharm. Sci.* 98, 565-572.

Mantaj, J., Jackson, P.J.M., Rahman, K.M. and Thurston, D.E., From Anthramycin to Pyrrolobenzodiazepine-Containing Antibody-Drug Conjugates (ADCs). *Angewandte Chemie*, **56**, 462–488 (2017). [DOI: 10.1002/anie.201510610]

Moghadam, S.H., Saliyaj, E., Wettig, S.D., Dong, C., Ivanova, M.V., Huzil, J.T., Foldvari, M., 2013. Effect of chemical permeation enhancers on stratum corneum barrier lipid organizational structure and interferon alpha permeability. *Mol. Pharm.* 10, 2248-2260.

Mohammed, D., Matts, P.J., Hadgraft, J., Lane, M.E., 2014. In vitro–in vivo correlation in skin permeation. *Pharm. Res.* 31, 394-400.

Oliveira, G., Hadgraft, J., Lane, M.E., 2012a. The influence of volatile solvents on transport across model membranes and human skin. *Int. J. Pharm.* 435, 38-49.

Oliveira, G., Hadgraft, J., Lane, M.E., 2012b. The role of vehicle interactions on permeation of an active through model membranes and human skin. *Int. J. Cosmet. Sci.* 34, 536–554.

Parisi, N., Paz-Alvarez, M., Matts, P., Lever, R., Hadgraft, J., Lane, M., 2016. Topical delivery of hexamidine. *Int. J. Pharm.* 506, 332-339.

Petrusek, R.L., Anderson, G.L., Garner, T.F., Fannin, Q.L., Kaplan, D.J., Zimmer, S.G., Hurley, L.H., 1981. Pyrrolo[1,4]benzodiazepine antibiotics. proposed structures and characteristics of the in vitro deoxyribonucleic acid adducts of anthramycin, tomaymycin, sibiromycin, and neothramycins A and B. *Biochemistry.* 20, 1111-1119.

Porter, W.H., Auansakul, A., 1982. Gas-Chromatographic determination of ethylene glycol in serum. *Clin. Chem.* 28, 75-78.

Pudney P.D., Mélot, M., Caspers, P.J., Van Der Pol, A., Puppels, G.J., 2007. An in vivo confocal Raman study of the delivery of trans retinol to the skin. *Appl. Spectrosc.* 61, 804-11.

Roussel, L., Abdayem, R., Gilbert, E., Pirot, F., Haftek, M. Influence of excipients on two elements of the stratum corneum barrier: intercellular lipids and epidermal tight junctions. In: *Percutaneous Penetration Enhancers Chemical Methods in Penetration Enhancement: Drug*

Manipulation Strategies and Vehicle Effects. (Editors: N. Dragicevic, H.I.Maibach).
Springer-Verlag. Berlin Heidelberg. 2015. p.80-81.

Santos, P., Machado, M., Watkinson, A.C., Hadgraft, J., Lane, M.E., 2009. The effect of drug concentration on solvent activity in silicone membranes. *Int. J. Pharm.* 377, 70-75.

Scientific Committee on Consumer Safety (SCCS), 2010. Basic criteria for the in vitro assessment of dermal absorption of cosmetic ingredients. SCCS/1358/10. 14 pages.

Sinco, P.J., Singh, Y., 2011. States of matter, 6th ed. Lippincott Williams and Wilkins, Baltimore, Philadelphia.

Subra, C., 2013. Diethylene glycol monoethyl ether, In: Rowe, R.C., Sheskey, P.J., Cook, W.G., Fenton, M.E. (Eds.), *Handbook of Pharmaceutical Excipients (Online Edition)*. Pharmaceutical Press and American Pharmacists Association.

Taylor, A.K., 2013. Isopropyl myristate, In: Rowe, R.C., Sheskey, P.J., Cook, W.G., Fenton, M.E. (Eds.), *Handbook of Pharmaceutical Excipients (Online Edition)*. Pharmaceutical Press and American Pharmacists Association.

Tendler, M.D., Korman, S., 1963. 'Refuin': a non-cytotoxic carcinostatic compound proliferated by a thermophilic actinomycete. *Nature*. 199, 501.

United States Environmental Protection Agency., 1996. *Product Properties Test Guidelines OPPTS 830.7550 Partition Coefficient (n-Octanol/Water), Shake Flask Method*, United States Environmental Protection Agency: 7: 1-9.

Table 1. GC analytical methods for solvents

Solvents→	PG	BD	TC	DiPG	PGMC	PGML	IPM
Column	HP 5	HP 5	Ultra 1	Ultra 1	Ultra 1	HP 5	HP 5
Injection volume (µl)	1	1	2	2	2	1	2
Split ratio	25	25	50	5	50	25	40
Flow rate (ml/min)	2	1.5	2	0.8	2	1.2	1
Inlet temperature (°C)	250	240	300	300	300	360	250
Detector temperature (°C)	300	280	250	250	250	300	300
Run time (min)	8	10	11	11	12.78	8	12
Initial temperature (°C)	100	120	120	110	100	100	125
Hold time at initial temp (min)	2	2	1	0	1	0	0
Final temperature (°C)	280	240	225	190	225	280	185
Ramp to final temperature (°C/min)	30	20	11.6	8	11.6	30	30
Hold time in final temp (min)	0	2	1	1	1	2	10

Table 2. Physicochemical properties of ANT.

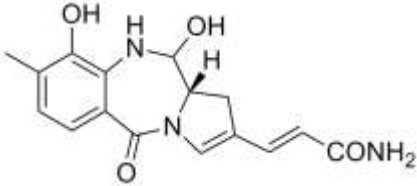
Chemical structure	
Molecular formula	: C ₁₆ H ₁₇ N ₃ O ₄
Molecular weight	: 315.32 Da
Log P	: 1.15±0.83
Melting point	: 188-194 °C (Leimgruber et al., 1965a)
Solubility parameter	: 15.35 (cal/cm ³) ^{1/2}

Table 3. Physicochemical parameters of candidate solvents

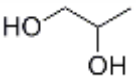
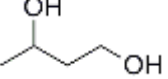
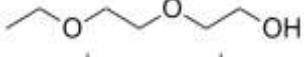
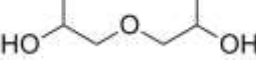
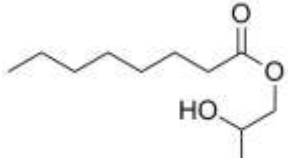
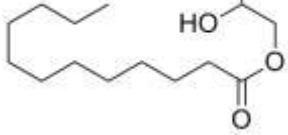
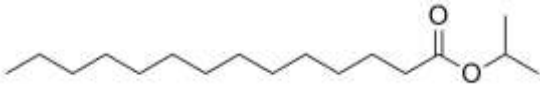
Solvent	Chemical structure	Molecular weight (Da)	Log P	Vapour pressure (mm of Hg)	Solubility parameter (cal/cm ³) ^{1/2}
PG		76.09	- 0.47	0.07 at 20 °C (Ladyzhynsky, 2013)	14.07
BD		90.14	- 0.37	0.06 at 20 °C (Fenton and Rowe, 2013a)	14.09
TC		134.17	- 0.25	0.12 at 20 °C (Subra, 2013)	10.62
DiPG		134.17	- 0.31	0.02 at 25 °C (Fenton and Rowe, 2013b)	12.19
PGMC		202.29	2.5	-	9.89
PGML		258.40 (Fenton and Rowe, 2013c)	4.17	-	9.44
IPM		270.45 (Taylor, 2013)	5.86	9.35E-05 at 25 °C (Daubert and Danner, 1989)	8.21

Table 4. Solubility of ANT in candidate vehicles at $32\pm 0.5^\circ\text{C}$ (n=3, mean \pm SD).

Vehicle	Solubility (mg/ml)
PG	172.93 \pm 28.39
BD	74.60 \pm 8.11
DiPG	67.26 \pm 14.22
TC	23.99 \pm 5.16
PGMC	5.60 \pm 0.90
PGML	5.65 \pm 0.70
IPM	0.24 \pm 0.04
Water	2.18 \pm 0.16

Table 5. Percentage of ANT recovered from skin surface, inside the skin and permeation into? (mean±SD, n≥3)

Percentage (%) of applied dose			
Solvent	From the surface	Inside the skin	Permeation
PG	80.1±3.2	1.3±0.7	0.6±0.1
TC	71.6±25.0	4.4±1.6	8.0±2.9
BD	102.3±9.6	0.3±0.1	0
DiPG	98.45±15.3	0.2±0.0	0
PGMC	73.8±16.8	17.5±8.2	0
PGML	75.1±21.4	4.0±1.0	13.1±0.4
IPM	0	59.2±7.1	0

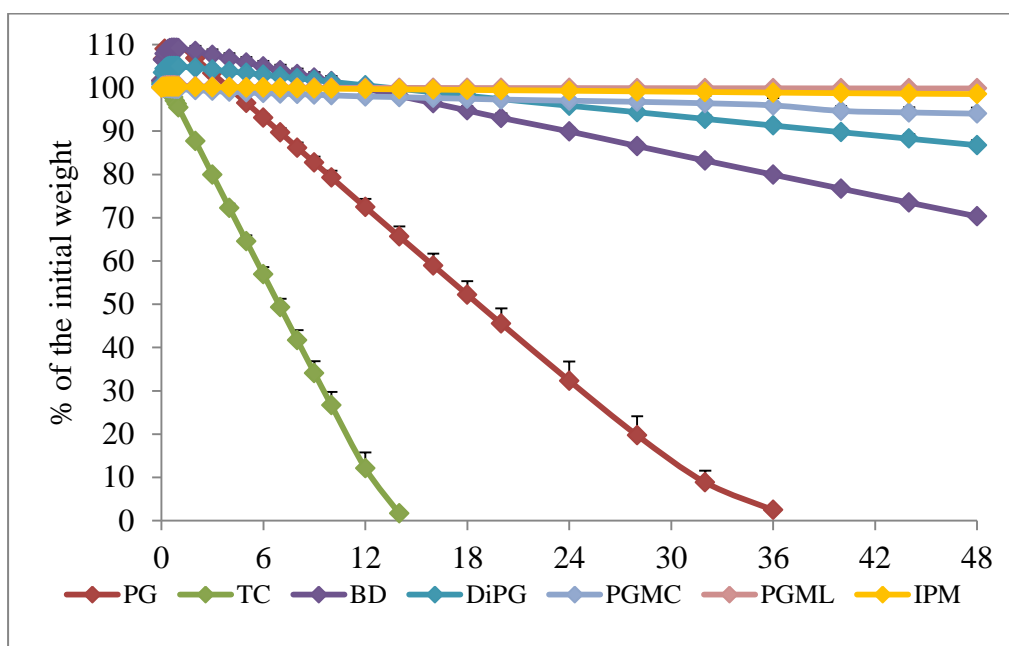


Figure 1. Percentage of the applied weight of solvents remaining as measured with Dynamic Vapor Sorption, over 48 h at $32 \pm 1^\circ \text{C}$ and $50 \pm 1.5\% \text{RH}$ ($n=3$, $\text{mean} \pm \text{SD}$)

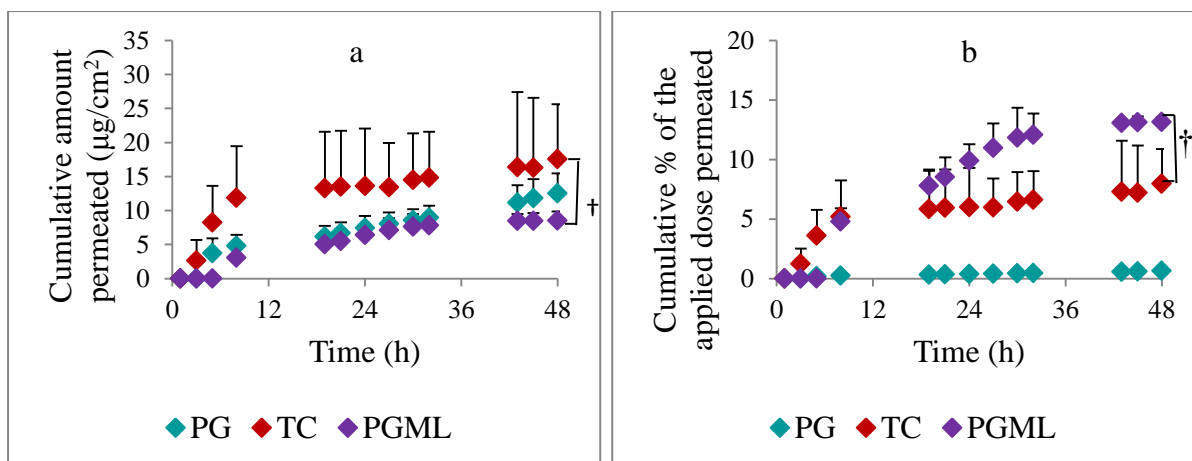


Figure 2. (a) Cumulative amount of ANT permeated ($\mu\text{g}/\text{cm}^2$) and (b) percentage of the applied dose of ANT permeated as a function of time (h) from single solvents across human skin ($n \geq 3$, mean \pm SD). (†) indicates $p > 0.05$.

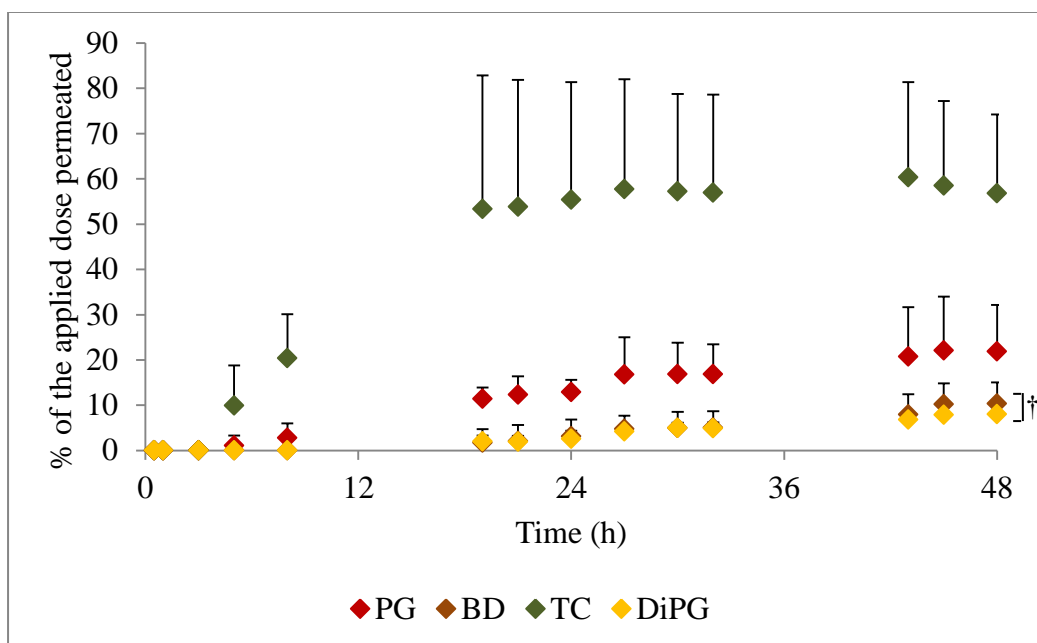


Figure 3. Percentage permeation of PG, BD, TC and DiPG across human skin vs. time ($n \geq 3$, mean \pm SD). (†) indicates no significant differences ($p > 0.05$).

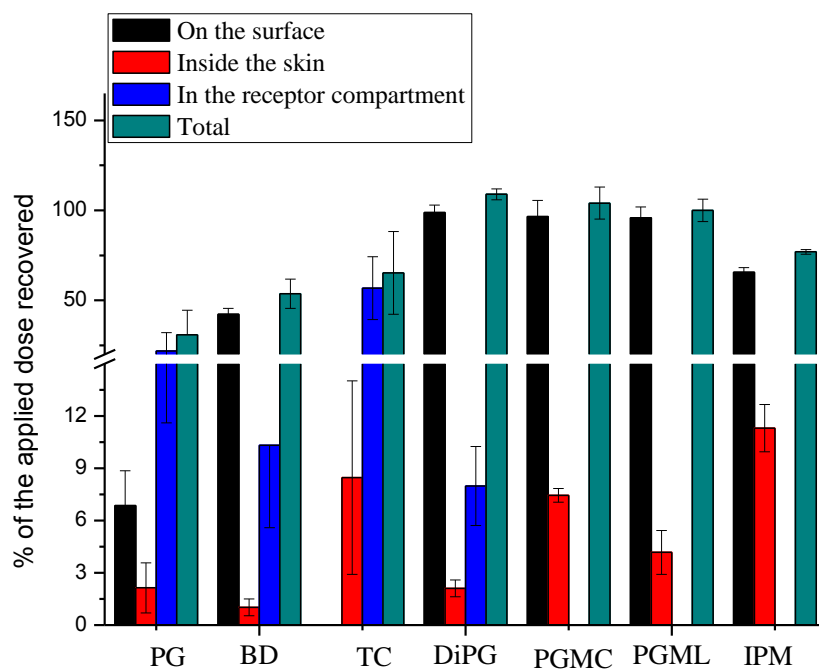


Figure 4: Percentages of solvents recovered from skin surface, inside the skin and permeated after 48 h permeation in human skin ($n \geq 3$, mean \pm SD).